

Spectral distribution in the reflection of parametric X-rays

This content has been downloaded from IOPscience. Please scroll down to see the full text.

2014 J. Phys.: Conf. Ser. 517 012018

(<http://iopscience.iop.org/1742-6596/517/1/012018>)

View [the table of contents for this issue](#), or go to the [journal homepage](#) for more

Download details:

IP Address: 82.151.111.206

This content was downloaded on 05/05/2015 at 16:06

Please note that [terms and conditions apply](#).

Spectral distribution in the reflection of parametric X-rays

Yu A Chesnokov¹, A V Shchagin^{2,3}, N F Shul'ga², A S Kubankin³,
A P Potylitsyn⁴, A S Gogolev⁴, S R Uglov⁴, Yu M Cherepennikov⁴, P Karataev⁵

¹ Institute of High Energy Physics, Moscow Region, Protvino, Russia;

² National Science Center "Kharkov Institute of Physics and Technology", Kharkov, Ukraine;

³ Belgorod State University, Belgorod, Russia;

⁴ Tomsk Polytechnic University, Tomsk, Russia;

⁵ John Adams Institute at Royal Holloway College, University of London, Egham, UK;

E-mail: kubankin@bsu.edu.ru

Abstract. The parametric X-ray radiation (PXR) spectra are measured on condition when the angular size of PXR cone is smaller than the angular resolution of the experiment. The PXR is generated under interaction of 50GeV proton beam with silicon crystal in Bragg geometry. The comparison of experimental data with results of developed theoretical model is presented and discussed.

1. Introduction

Parametric X-ray radiation (PXR) appears due to the Bragg diffraction of a fast charged particle Coulomb field on a system of atomic planes in a crystal [1-5]. The PXR of relativistic charged particles in crystals has been studied theoretically and experimentally (see, for example, reviews of some experimental research in Refs. [1, 2]). In particular, the PXR excited by relativistic protons in crystals has been observed in Refs. [3 – 5].

The PXR spectrum in symmetrical diffraction geometry consists of peaks corresponding to different orders of the diffraction. The shape and spectral width of peaks are determined by angular sizes of detector, and transverse cross-section of incident particle beam, and the incident beam divergence. These parameters determine the angular resolution in PXR experiments. The shape of the PXR spectral peaks can be substantially modified when the angular resolution is comparable with the PXR cone angle.

The presented research is devoted to the study of PXR spectral distribution under conditions when the experimental angular resolution is comparable with the angular size of the PXR reflection. The experiment was performed at the proton accelerator U70 of the Institute of High Energy Physics, Protvino, Russia. The methods for PXR measuring are developed for conditions of intense background radiation of fast charged particles and X-rays. The measurement results and calculations are in good accordance to each other. The PXR model is developed on the base of kinematical theory of PXR [6]. The relativistic system of units $\hbar = c = 1$ is used in the theoretical part of the work.



It should be noted that the presented results are the preparation stage for the comprehensive research of effects of focusing of the PXR emitted from a bent crystal [7].

2. Calculations

The kinematical model of PXR [6] is used below in calculations of the PXR properties, in spite that it does not describe the asymmetry of the yield in the PXR reflection [8]. According to calculations the position of the PXR peak is about at energy $\omega \approx 10.9\text{keV}$ for the observation angle of the beam 20° that corresponds to the present experimental setup geometry which is described in details below. The mechanisms of the transition radiation and bremsstrahlung are realized also in process of protons interaction with the target. The yield of the transition radiation is negligible in condition $\omega \gg \gamma\omega_p \approx 1.8\text{keV}$, where $\gamma\omega_p$ determines the threshold of intense transition radiation manifestation (ω_p is the plasma frequency of the target, γ is the Lorentz factor of an emitting particle). This circumstance means that the contribution of the transition radiation is negligible. The contribution of the bremsstrahlung is also negligibly because of its small intensity for heavy particles.

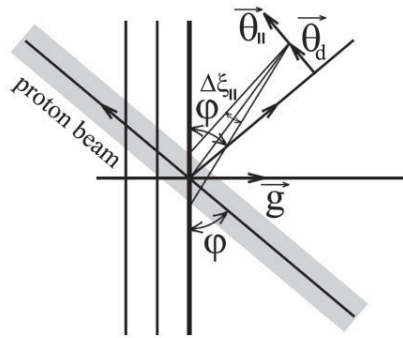


Figure 1. The radiation process geometry.

The radiation process geometry for the finite transverse size of the particle beam can be considered as presented in figure 1, where φ is the incidence angle of the particle beam on the crystallographic plane determined by reciprocal lattice vector \mathbf{g} , the angles θ_d and θ_{\parallel} determine the detector position and observation angle in the incidence plane relative to the direction of mirror reflection of the particle beam, $\Delta\xi_{\parallel}$ is the angular size of the beam cross section in the incidence plane. The variables θ_{\perp} and $\Delta\xi_{\perp}$ mean the same that θ_{\parallel} and $\Delta\xi_{\parallel}$ but at transverse direction (normally to the incidence plane). The spectral-angular distribution of PXR for a single proton can be presented in a convenient form for the future calculations

$$\omega \frac{d^3 N}{d\omega d\theta_{\parallel} d\theta_{\perp}} = \frac{e^2 \omega_g^4}{\pi g^2} \frac{1}{\omega \chi_0''(\omega)} \frac{\tan(\varphi)}{\omega_B} F(\theta_{\parallel}, \theta_{\perp}, \omega, \varphi) \delta \left[\theta_{\parallel} + \left(1 - \frac{\omega}{\omega_B} \right) \tan(\varphi) \right], \quad (1)$$

$$F(\theta_{\parallel}, \theta_{\perp}, \omega, \varphi) = \frac{\theta_{\perp}^2 + \theta_{\parallel}^2 \cos^2(2\varphi)}{(\gamma^{-2} + \omega_0^2/\omega^2 + \theta^2)^2},$$

where $\varepsilon(\omega) = 1 - \omega_p^2/\omega^2 + i\chi''(\omega)$ is the average dielectric permeability of the crystal, $\omega_B = g/2\sin(\varphi)$

is the Bragg frequency, $\omega_g^2 = \omega_p^2 (F(g)/Z)(S(\vec{g})/N_0) \exp(-g^2 u_T^2)$, $F(g)$ is the formfactor of an atom, Z is the number of electrons in the atom, $S(\vec{g})$ is the structure factor of an elementary cell containing N_0 atoms, u_T is the mean-square amplitude of thermal vibrations of atoms, other variables are determined in figure 1.

The PXR is realized in conditions of large transverse size of proton beam and distribution (1) must be averaged by the detector observation angles for each proton in the beam. The averaging can be performed taking into account that angular size of PXR cone is substantially larger than the angular size of the detector aperture determined by the ratio d/L , where d is the aperture size, L is the distance from the detector to the point of PXR process. The maximum of the PXR angular distribution is realized at angles $\pm\sqrt{\gamma^{-2} + \omega_0^2/\omega^2} = \pm 19$ mrad in the given geometry, whereas $d/L \approx 9.5$ mrad. This feature allows to substitute the integration of the PXR spectral-angular distribution over angular detector size $\Delta\theta_\perp$ by multiplication of the distribution on $\Delta\theta_\perp$.

The averaged spectral-angular distribution of PXR can be presented in the form

$$\left\langle \omega \frac{d^3 N}{d\omega d\theta_\parallel d\theta_\perp} \right\rangle = \frac{e^2 \omega_g^4}{\pi g^2} \frac{1}{\omega \chi_0''(\omega)} \frac{1}{\omega_B \cot(\varphi)} \frac{\Delta\theta_\perp}{\Delta\xi_\perp \Delta\xi_\parallel} \times \int_{\frac{-\Delta\xi_\parallel}{2}}^{\frac{\Delta\xi_\parallel}{2}} \sigma\left(\frac{\Delta\theta_\parallel}{2} + \xi_\parallel - \theta_d + \theta^*\right) \sigma\left(\frac{\Delta\theta_\parallel}{2} - \xi_\parallel + \theta_d - \theta^*\right) \int_{\frac{-\Delta\xi_\perp}{2}}^{\frac{\Delta\xi_\perp}{2}} F(\theta^*, \xi_\perp, \omega, \varphi) d\xi_\parallel d\xi_\perp. \quad (2)$$

where $\theta^* = (1 - \omega/\omega_B) \tan(\varphi)$, $\Delta\theta_\perp$ and $\Delta\theta_\parallel$ are the transverse and longitudinal angular sizes of the detector aperture, $\sigma(x)$ is the Heaviside step function. The expression (2) is valid for the rectangular beam cross-section. For other shapes of the cross-section the averaging must be performed with a function of cross-section current density.

The shape of PXR spectral peak can be modified substantially on condition when $\Delta\xi_\parallel$ size of order $\sqrt{\gamma^{-2} + \omega_0^2/\omega^2}$. The figure 2 presents dependences of the shape on the angular beam size $\Delta\xi_\parallel$. The curve 2 corresponds to case when the angular sizes of the beam cross section in the incidence plane equal to PXR cone angular size ($\Delta\xi_\parallel = 2\sqrt{\gamma^{-2} + \omega_0^2/\omega^2}$). It is shown the modification of the shape of PXR peak to two-hump shape. The size $\Delta\xi_\perp$ determines the magnitude of the effect and it is decreased if $\Delta\xi_\perp$ increases, that is presented in figure 3.

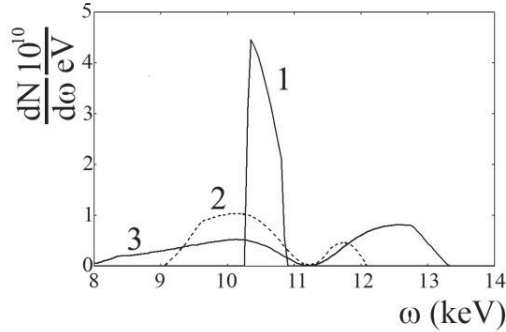


Figure 2. The dependence of PXR on radiating particle beam size $\Delta\xi_{||}$. The curves are calculated at parameters $\Delta\theta_{\perp}=8.4$ mrad, $\Delta\theta_{||}=8.4$ mrad, $\varphi=170$ mrad, $\Delta\xi_{\perp}=5$ mrad, $\gamma=54$, $\theta_d=-10$ mrad. 1 – $\Delta\xi_{||}=1$ mrad, 2 – $\Delta\xi_{||}=38$ mrad, 3 – $\Delta\xi_{||}=76$ mrad.

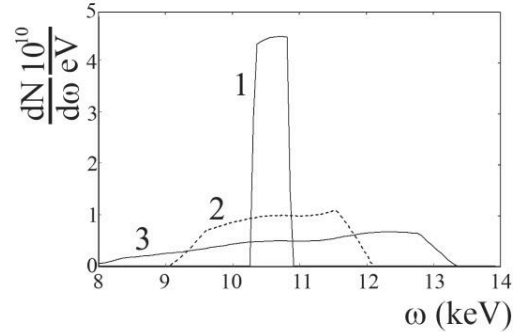


Figure 3. The influence of angular transverse size of the beam cross-section on PXR. The parameters are the same that for the figure 2 except $\Delta\xi_{\perp}=92$ mrad.

The proton beam dimensions (FWHM) in the setup geometry were about 25 mm in the vertical direction and 10 mm in the horizontal direction that corresponds to angular sizes of beam observation $\Delta\xi_{\perp}=100$ mrad and $\Delta\xi_{||}=40$ mrad in geometry of the calculations for (2). Both angular sizes exceed typical angular size of the PXR manifestation for 50 GeV protons.

3. Experimental

The experiment has been performed at extracted 50 GeV proton beam in accelerator U70. The setup is presented schematically in figure 4. The beam was extracted from U70 orbit by a Si crystal bent on 90 mrad. The intensity of the extracted beam was about 10^7 protons per pulse. The beam time structure

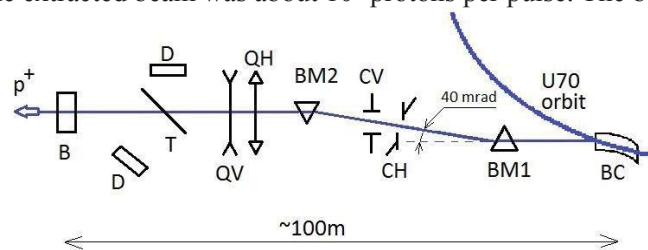


Figure 4. The experimental setup.

was one pulse duration 1s every 10s. The extraction is well described in [9]. The extracted beam is parallel shifted by the 6-m long bending magnets BM1 and BM2 for the beam clearing of the background generated during extraction. The copper collimators CH and CV of length 75 cm form a rectangular shape of the proton beam. The 2-m long quadrupole lenses (QH and QV) provide the beam divergence of about 100 μ rad in both horizontal and vertical planes. The PXR was produced under interaction of the formed beam with the 300 μ m thick Si (111) target T, mounted on a goniometer with step of $2.18 \cdot 10^{-5}$ rad. The goniometer, the target and the X-ray detector were assembled in air. The proton beam propagated from

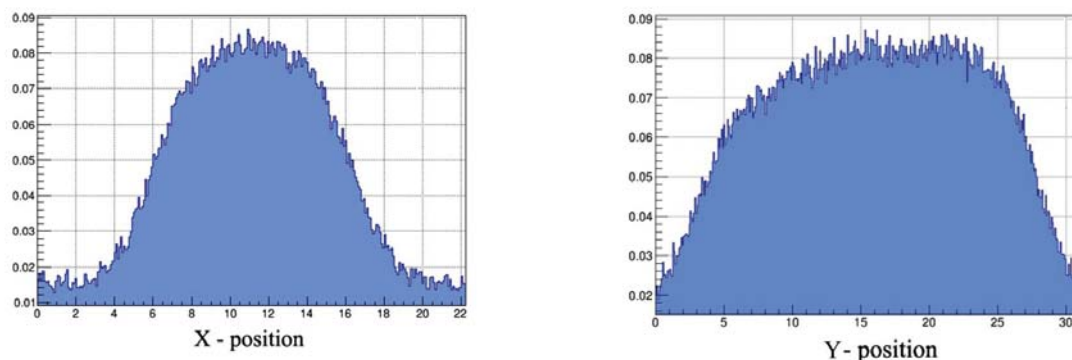


Figure 5. The proton beam profile in the vicinity of the target.

the vacuum tube to air through a Mylar foil. The distance from the Mylar foil to the target was about 1 m. The proton beam profile measured in the vicinity of the target is shown in figure 5. The measurements were performed using the Dosimetry Film EBT2 and a scanner with a resolution of $20\ \mu\text{m}$.

The number of protons in the beam is counted by a fast scintillator counter B. The energydispersive PIN detector XR-100CR and a digital pulse processor PX4 (both from Amptek) were used for PXR and background measurements. The detector has $500\ \mu\text{m}$ thick Si crystal with the area of $6\ \text{mm}^2$ equipped with a 0.3 mil Be window. An inner collimator of detector crystal has the aperture of $4.4\ \text{mm}^2$. The collimator is opaque for soft X-rays but transparent for hard X-rays and relativistic particles. Due to intense background radiation we applied the shortest available in the PX4 peaking time $0.8\ \mu\text{s}$. The energy resolution of the spectrometer is about 260 eV at X-ray energy 5.9 keV. The applying of the small gain in spectrometer allows observing the intense background occurring as a consequence of the energy losses of charged particles in the detector crystal.

At the first stage, the radiation of the Cu characteristic lines at energies 8.04keV and 8.93keV was measured to test the spectroscopy equipment characteristics and to measure the background level relative to Cu characteristic radiation. A $20\ \mu\text{m}$ thick Cu foil was used as the target. The surface of the Cu foil was oriented at angle 45° relative to the proton beam. The detector was installed at angle 90° relative to the proton beam at the 60cm distance from the target. The measurement showed a continuous background appearing in soft and hard X-ray regions of PX4 multichannel analyzer. The soft background part corresponds to radiation processes at interaction of primary protons and secondary charged particles with a medium. The spectrum of this part is in the range up to 10keV. The background mechanism at the hard region corresponds to ionization losses of charged particles in the detector crystal. The intensity of this background is depended on the distance between the detector and the proton beam and in general does not depend on the target material.

The Si (111) target $300\ \mu\text{m}$ thick was used for PXR observation. The detector D was installed at observation angle 19.9° at distance 25 cm away from the target. The measurement accuracy of the incidence angle and the distance was in the range $\pm 1.2^\circ$ and $\pm 15\text{mm}$ that is explained by the large size of the particle beam (these estimations for the transverse FWHM of the beam in incidence plane 10 mm). The angle and position of the detector installation were chosen for PXR observation on condition of weak background manifestation that allows to measure clear signal in PXR spectral range. The Si target was mounted on the goniometer and preliminarily aligned for observation of the PXR in Bragg geometry. The experimental setup for the PXR studies is shown in figure 6.

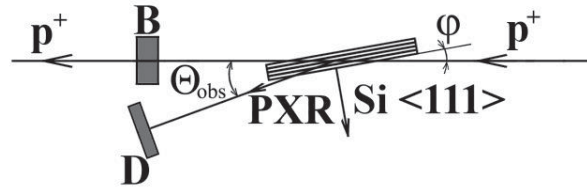


Figure 6. The setup for the PXR measurements.

4. Results and discussion

The PXR spectrum was measured for two orientations of the crystal. The first measurement was done for $\varphi=9.95^\circ$ and $\Theta_{obs}=19.9^\circ$. The comparison of the measurement with calculation is shown in figure 7. The dotted graph includes the possible correction for the observation and incidence angles in frames of the measurement accuracy mentioned above ($\varphi=11.2^\circ$ and $\Theta_{obs}=22.4^\circ$).

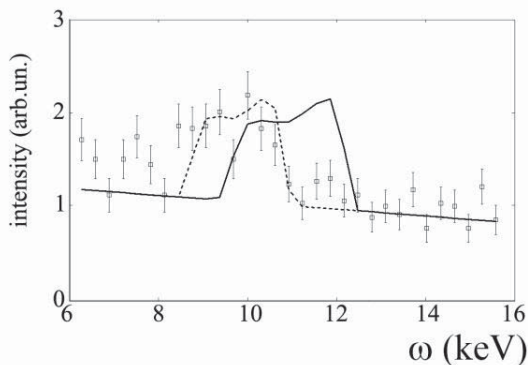


Figure 7. The comparison of the PXR measurement with calculation for the angles $\Theta_{obs}=19.9^\circ$, $\varphi=9.95^\circ$ and $\Theta_{obs}=22.4^\circ$, $\varphi=11.2^\circ$ (dotted graph).

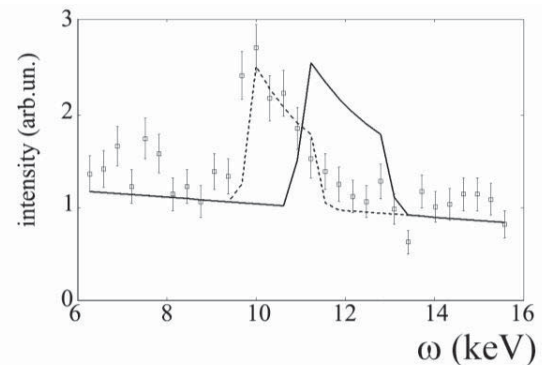


Figure 8. The comparison of the PXR measurement with calculation for the angles $\Theta_{obs}=19.9^\circ$, $\varphi=11.45^\circ$ and $\Theta_{obs}=22.4^\circ$, $\varphi=12.7^\circ$ (dotted graph).

The second measurement was done at the same observation angle Θ_{obs} , but for $\varphi=11.45^\circ$. The result is presented in figure 8. The dotted graph is in condition of Θ_{obs} correction like to the dotted graph in figure 7 ($\Theta_{obs}=22.4^\circ$, $\varphi=12.7^\circ$).

In present paper we demonstrated both theoretically and experimentally that the shape of the PXR spectral distribution can possess a complicated form if the experimental angular resolution exceeds the angular size of the PXR reflection. In particular, the distribution can have two maxima and the energy in the maxima can be different from the PXR energy calculated for average observation angle. This situation is completely different from the case when the experimental angular resolution is well below of the angular size of the PXR reflection and the PXR spectral distribution is quasi-monochromatic.

Presented here preliminary calculated and experimental data on the PXR spectral distributions are in satisfactory agreement one to another at deviation of the observation angle for 2.5° . But we have to note poor statistics and high level of radiation background in the experiment as well as that the asymmetry of the yield in the PXR reflection was not taken into account in calculations. In more detail research one has to obtain the experimental data with reduced level of background radiation, and with better statistics, and

with more exactly determined experimental geometry and compare results of measurements to calculations performed with proper account of the asymmetry of the yield in the PXR reflection [8].

Acknowledgements

The joint research is supported by the directorates of the IHEP and KIPT. The activity of participants from Protvino and Kharkov was supported by joint Russian-Ukrainian Grants by the RFBR Grant № 13-02-90434 (Russia) and by the SFFR Grant № F53.2/107 (Ukraine). The participants from Tomsk acknowledge the partial support by the Ministry of education and science of the Russian Federation grant № 14.B37.21.0912 and the RFBR Grant № 13-02-31090.

References

- [1] Shchagin A V, Maruyama X K 1997 *Parametric X-rays Accelerator-Based Atomic Physics Techniques and Applications* (AIP Press, New York) ed S.M. Shafroth and J.C. Austin 279
- [2] Potylitsyn A P 2011 *Electromagnetic Radiation of Electrons in Periodic Structures* (Springer-Verlag, 243)
- [3] Afanasenko V P et al. 1992 *Phys. Lett. A* **170** 315
- [4] Adishchev Yu N, Artemov A S, Afanasiev S V et al. 2005 *JETP Lett.* **81** 241
- [5] Scandale W et al. 2011 *Phys. Lett. B* **701** 180
- [6] Feranchuk I, Ivashin A 1985 *J. Phys. (Paris)* **46** 1981
- [7] Shchagin AV 2004 *JETP Lett.* **80** 469
- [8] Shchagin A V, Takabayashi Y 2013 *Nucl. Instr. and Meth. in Phys. Res. B* **309** 198
- [9] Arkhipenko A A et al. 2008 *JETP Lett.* **88** 229